Pure & Appl. Chem., Vol. 67, No. 3, pp. 463–472, 1995.
Printed in Great Britain.

Spectroscopy of spin-polarized excitons in semiconductors

E.L. Ivchenko

A.F.Ioffe Physico-Technical Institute, Politechnicheskaya 26, 194021 St.Petersburg, Russia

ABSTRACT

Excitons in semiconductors can be spin-polarized under optical selective excitation by polarized radiation (optical orientation) or due to spin relaxation and sublevel mixing in an external magnetic field. The paper deals with optical phenomena where spin-polarized excitons generated in semiconductor nanostructures play an important role. Firstly, both optical orientation and optical alignment of excitons in type II GaAs/AlAs superlattices are considered and effects of the anisotropic electron-hole exchange interaction and external magnetic field on the photoluminescence polarization are analyzed. Secondly, magnetic-field-induced anticrossing of excitonic sublevels is discussed taking into account the axial and anisotropic exchange splittings, spin-relaxation and difference in the lifetimes of radiative and non-radiative exciton states. Next, the localized and bound excitons are shown to act as intermediate states in resonant Raman scattering by spin flips of holes bound to acceptors in GaAs/AlGaAs multiple quantum wells. The analysis of polarized Raman spectra permits to make decisive conclusions concerning microscopic mechanisms of the observed scattering prosesses. Finally, the doubly-resonant 2s-1s LO-assisted secondary emission observed in CdTe/CdMnTe quantum-well structures is described as a process with spin-polarized hot 1s-excitons acting as real intermediate states.

1. INTRODUCTION

The exciton spin polarization in bulk semiconductors was extensively studied in 70-ies and early 80-ies (see the review[1] and references therein). In the absence of an external magnetic field spin-polarized excitons can be generated under optical pumping with circularly polarized photons: due to spin-orbit coupling of electronic states the selection rules for optical interband transitions provide a conversion of photon polarization into photocarrier or exciton spin orientation. In accordance with the selection rules the radiative recombination of spin-polarized excitons results in the circular polarization of the photoluminescence thus making possible optical detection of the spin polarization. The optical orientation of excitonic spins is a particular case of the more general phenomenon, namely, the selective optical excitation of excitonic sublevels. Another example of the selective excitation is the so-called optical alignment of excitons by linearly polarized radiation: in contrast to the optical orientation which means just the photoinduced difference in the populations of the exciton states $|m>$ with the spin $m = \pm 1$, the linearly-polarized light can excite preferentially the exciton state $(|+1> + e^{i\Phi}|-1>)/\sqrt{2}$ with a definite direction of oscillating electric-dipole moment (a value of the phase Φ is determined by the direction of the light polarization plane). Application of an external field (magnetic field, strain) reduces symmetry of the system and can lead to interconnection between exciton optical orientation and alignment in which case it is necessary to consider not only circular-circular and linear-linear but also mixed circular-linear or linear-circular configurations of the polarizer and analyzer.

The optical orientation effect can be readily observed if the spin relaxation time, τ_s, is not too small relative to the exciton lifetime, τ. If however $\tau_s \ll \tau$ a more convenient method is to observe the thermal orientation of spins in a magnetic field: due to spin relaxation upper and lower split sublevels become selectively populated even under unpolarized excitation. There exist also non-thermal mechanisms of exciton spin polarization under unpolarized excitation, they are connected with magnetic-field-induced mixing and anticrossing (see e.g.[2]) of excitonic sublevels.

The present paper touches various aspects of the exciton spin polarization in semiconductor nanostructures. Optical selective excitation of excitonic sublevels in type II superlattices is considered in Section 2. The results on optically-detected exciton level-anticrossing in an external magnetic field are presented in Section 3. Bound and localized spin-polarized excitons acting as intermediate states in resonant Raman spin-flip scattering processes are analyzed in Section 4. Section 5 is devoted to optical orientation of hot excitons and their involvement in the doubly-resonant $2s - 1s$ secondary emission observed recently in CdTe/$Cd_{1-x}Mn_xTe$ quantum well structures[3].

2. OPTICAL ORIENTATION AND ALIGNMENT OF EXCITONS IN GaAs/AlAs SUPERLATTICES

We show the efficiency of optical selective excitation methods on GaAs/AlAs(001) superlattices which are a convenient model object to study type I - type II transitions in heterostructures. Really, depending on the layer thicknesses the bottom of the conduction band in these structures is formed mainly either from states of the Γ-minimum in the GaAs layer (type I) or from states of the X-minimum in the AlAs layer (type II). The lowest excitonic level $e1-hh1(1s)$ in both types consists of four sublevels taking into account the electron ($\pm 1/2$) and heavy hole ($\pm 3/2$) spin degeneracy. Symmetry considerations show that, in an ideal structure, due to the electron-hole exchange interaction the exciton state is split into a radiative doublet and two close-lying non-radiative sublevels.

However experiments on polarized luminescence resonantly excited by circularly or linearly polarized light[4,5] and on optically detected magnetic resonance[6] showed that, for localized excitons in type II GaAs/AlAs superlattices, (i) the degeneracy of the radiative doublet is lifted, (ii) the two split sublevels are dipole-active along the [110] and [1$\bar{1}$0] directions in the layer plane, and (iii) in a single superlattice with fixed layer thicknesses two classes of excitons can be excited simultaneously with the same value but opposite signs of the anisotropic exchange splitting. In [7] we have explained the nature of this giant anisotropic splitting taking into account the mixing of heavy and light hole states on the interfaces and connecting the two classes of localized excitons with those attached to the GaAs/AlAs and AlAs/GaAs interfaces. The recent numerical calculations[8] have confirmed the proposed idea about considerable heavy-light hole mixing by the (001) inteface at normal incidence of the hole.

Optical orientation and alignment of excitons can be described by using the density matrix formalism[1,5,9]. In a steady-state regime of photoexcitation, the components $\rho_{jj'}$ of the localized-exciton density matrix satisfy the kinetic equation

$$\left(\frac{\partial\rho}{\partial t}\right)_{rec} + \left(\frac{\partial\rho}{\partial t}\right)_{s.r.} + \frac{i}{\hbar}\left[\rho, \mathcal{H}_{exch} + \mathcal{H}_{\mathbf{B}}\right] = G\,. \tag{1}$$

The terms on the left-hand side take account of the exciton recombination, spin relaxation, exchange and Zeeman interaction in the presence of magnetic field $\mathbf{B}$, G is the generation matrix. Let $|m\rangle_0$ be the basis states of the $e1 - hh1(1s)$ exciton with the angular momentum component $m = s_z + J_z = \pm 1, \pm 2$. In this basis the exchange term in the spin Hamiltonian is given by

$$\mathcal{H}_{exch} = \frac{1}{2}\begin{bmatrix} \delta_0 & i\delta_2 & 0 & 0 \\ -i\delta_2 & \delta_0 & 0 & 0 \\ 0 & 0 & -\delta_0 & \delta_1 \\ 0 & 0 & \delta_1 & -\delta_0 \end{bmatrix}, \tag{2}$$

where δ_n are the exchange interaction constants[7] with δ_2 describing the above-mentioned anisotropic exchange splitting. The recombimation term has a standart form

$$\frac{\partial\rho_{mm'}}{\partial t} = -\left(\frac{1}{\tau_m} + \frac{1}{\tau_{m'}}\right)\rho_{mm'}, \frac{1}{\tau_m} = \frac{1}{\tau_r}\delta_{|m|,1} + \frac{1}{\tau_0}\,, \tag{3}$$

where $\delta_{j,j'}$ is the Kronecker symbol, τ_r is the radiative lifetime for the exciton states $|\pm 1\rangle_0$, τ_0^{-1} is the non-radiative recombination rate which is usually assumed to be the same for all states.

Neglecting for simplicity the exciton spin relaxation we obtain for the photoluminescence circular polarization under resonant circularly-polarized excitation in the longitudinal magnetic field

$$P_c(\mathbf{B} \parallel z) = P_c^0 \frac{1 + \Omega_\parallel^2\tau^2}{1 + \left(\Omega_\parallel^2 + \tilde{\omega}^2\right)\tau^2}\,, \tag{4}$$

where z is the growth direction of the structure, $\tilde{\omega} = \delta_2/\hbar$, $\hbar\Omega_\parallel = (3g_h - g_e^\parallel)\mu_0 B_z$, $g_e^\parallel$ is the electron longitudinal g-factor, g_h is the heavy-hole g-factor defined so as the hole Zeeman energies are given by $\pm 3/2 g_h \mu_0 B$, μ_0 is the Bohr magneton, $\tau \equiv \tau_{\pm 1}$, P_c^0 is the circular polarization degree of the incident light. In type II GaAs/AlAs superlattices the anisotropic splitting exceeds the value of $\hbar/\tau$ so that $(\tilde{\omega}\tau)^2 \gg 1$ and at zero magnetic field the photoluminescence is practically unpolarized. The longitudinal magnetic field supresses the depolarizing effect of anisotropic exchange interaction and permits to observe the optical orientation of excitons (see Fig.1).

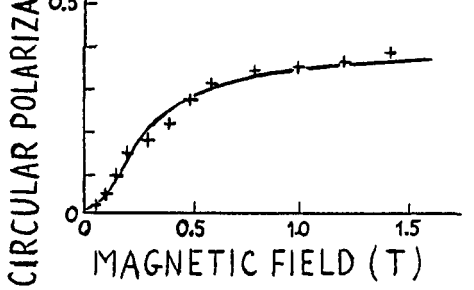

Fig. 1 Restoration of circular polarization of the $e1 - hh1$ exciton luminescence in the presence of the longitudinal magnetic field. Crosses are experimental points, solid curve is calculated by using equation $P_c \propto 1 - [1 + (B/B_{1/2})^2]^{-1}$ with $B_{1/2} = 0.25$ T. [5]

Eq.(4) describes relative radiation intensities only for circular-circular polarization configurations. A complete set of relations between polarizations of the incident and secondary radiations can be presented in the following form

$$P_c = \frac{\left(1+\Omega_\parallel^2\tau^2\right)P_c^0 - \Omega_\parallel\tilde{\omega}\tau^2 P_l^0 + \tilde{\omega}\tau P_{l'}^0}{1+\left(\Omega_\parallel^2+\tilde{\omega}^2\right)\tau^2}, \tag{5}$$

$$P_l = \frac{-\tilde{\omega}\Omega_\parallel\tau^2 P_c^0 + \left(1+\tilde{\omega}^2\tau^2\right)P_l^0 + \Omega_\parallel\tau P_{l'}^0}{1+\left(\Omega_\parallel^2+\tilde{\omega}^2\right)\tau^2}, \tag{6}$$

$$P_{l'} = \frac{-\tilde{\omega}\tau P_c^0 - \Omega_\parallel\tau P_l^0 + P_{l'}^0}{1+\left(\Omega_\parallel^2+\tilde{\omega}^2\right)\tau^2}, \tag{7}$$

Here P_l and $P_{l'}$ are the degrees of linear polarization referred respectively to the rectangular axes $x \parallel [1\bar{1}0]$, $y \parallel [110]$ and $x' \parallel [100]$, $y' \parallel [010]$:

$$P_l = \frac{I_x - I_y}{I_x + I_y}, \; P_{l'} = \frac{I'_x - I'_y}{I'_x + I'_y}.$$

the superscript 0 indicates polarization of the incident light.

The following additional conclusions can be made from the analysis of Eqs.(5-7): (1) For large anisotropic splitting, $\tilde{\omega} \gg \tau^{-1}$, the polarization $P_{l'}$ is negligibly small irrespective to the incident light polarization and magnetic field value. (2) At zero field, the excitons can be aligned under optical pumping in the polarization $\mathbf{E} \parallel x$ or y in agreement with the above-mentioned fact that the split radiative sublevels are polarized along the $[1\bar{1}0]$ and $[110]$ directions. (3) The magnetic-field-induced depolarization of optical alignment is described by the Lorentz-type curve with the halfwidth $B_{1/2} = |\delta_2/(3g_h - g_e^\parallel)\mu_0|$ which also governs the restoration of P_c. (4) Eqs.(5-7) give the polarization as a function of the magnetic field B_z for excitons with fixed sign of $\tilde{\omega}$. If excitons of both classes are taken into consideration the $\tilde{\omega}$-odd polarization degrees should be reduced because of the compensation. In the absence of complete compensation, i.e. if the densities of states for the two classes of localized excitons differ from each other, the circular-to-linear or linear-to-circular conversion can take place with the effect being maximal at $B = B_{1/2}$. The spin relaxation processes modify the 6x6 matrix connecting P_c, P_l, $P_{l'}$ with P_c^0, P_l^0, $P_{l'}^0$ but anyhow the main conclusions hold valid.

The time-resolved polarized photoluminescence can be also analyzed in the frame of the density-matrix formalism by adding to the left-hand side of Eq.(1) the time derivative $d\rho/dt$. Due to the anisotropic splitting between the $[1\bar{1}0]$– and $[110]$–polarized sublevels the selective excitation of localized excitonic states with a $< 100 >$ polarized light is followed by polarization quantum beats with the period $T_b = 2\pi\hbar/|\delta_2|$. This enables one to make the most direct measurements of the splitting δ_2 . The experimental values of δ_2 measured by optically detected magnetic resonance and quantum beats techniques are presented in Fig.2 together with the theoretical curves. The similar quantum beats can be excited with a circularly polarized light pulse. Moreover, in the case of two classes of excitons with different populations the circular polarization oscillation coexists with an appearance and $\pi/2$-phase-shifted oscillation of linear polarization $P_{l'}$ in a similar fashion as the circular and linear polarizations coexist in the light wave propagating perpendicularly to the principal axis of a birefringent medium. The transverse magnetic field $\mathbf{B} \perp z$ couples the radiative and non-radiative states in which case two periods are observed in the quantum beats the long and short periods corresponding to the small and large splitting energies of the excitonic quartet[10] .

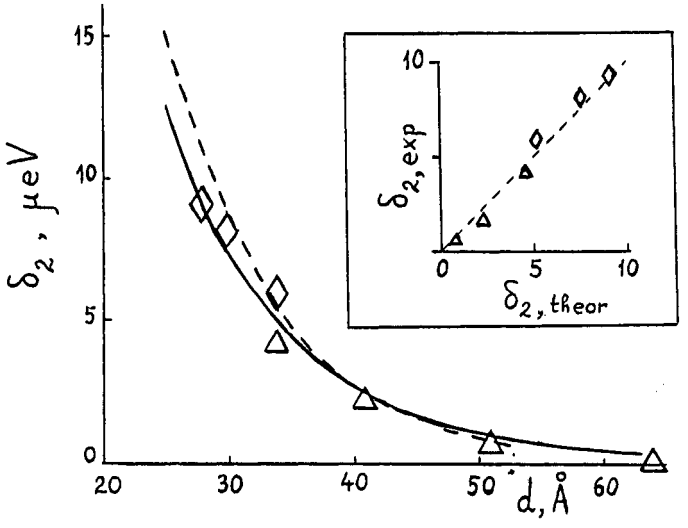

Fig. 2 Anisotropic exchange splitting of the radiative doublet as a function of the GaAs/AlAs superlattice period. Triangles[6] and rhombes[4] show experimental results, solid and dashed curves are calculated by using slightly different models[7].

3. OPTICALLY DETECTED EXCITON LEVEL-ANTICROSSING

This section responds to the experiment[11] and extends the theory of optically-detected anticrossing of excitonic levels in the longitudinal magnetic field, $\mathbf{B} \parallel z$, from bulk crystals [2] to superlattices. The preliminary results have been reported in [9].

The energies of the Zeeman-split quartet are given by

$$E_{1,2} = \frac{1}{2}[\delta_0 \pm \sqrt{\delta_2^2 + (3g_h - g_e^{\parallel})^2 \mu_0^2 B^2}] \ , \ E_{3,4} = \frac{1}{2}[-\delta_0 \pm (3g_h + g_e^{\parallel})\mu_0 B] \ .$$

At zero magnetic field the states 1, 2 are the [110]- and [1$\bar{1}$0]-polarized excitons, the sublevels 3, 4 coincide with the above basis excitonic states $|\pm 2\rangle_0$ since zero-field splitting between them is hereafter neglected ($\delta_1 = 0$). At two particular values of B the E_3 level crosses the levels E_1 and E_2. Near the crossing points the states 1, 3 or 2, 3 can be strongly mixed even by a weak symmetry-breaking potential V that couples radiative and non-radiative states. This effect known as the level-anticrossing can lead to a remarkable non-thermal exciton spin polarization under unpolarized excitation. One can set for the matrix elements of this perturbation

$$V_{m,m'} = V_0 \eta_{mm'} \ , \ \eta_{mm'} = \delta_{|m-m'|,1} \tag{8}$$

which corresponds to the presence of a small transverse magnetic-field component, $\mathbf{B}_\perp$. In this case the anticrossing parameter, V_0, is proportional to the electron transverse g-factor, $g_e^{\perp}$, because for heavy holes $g_h^{\perp} = 0$. Similarly, one can also consider the anticrossing mechanism due to static distortions mixing the heavy-hole states $\pm 3/2$ in which case $\eta_{mm'} = \delta_{|m-m'|,3}$. It is convenient to expand the eigenstates $|j\rangle$ ($j = 1 - 4$) of the spin Hamiltonian $\mathcal{H} = \mathcal{H}_{exch} + \mathcal{H}_{\mathbf{B}} + V$ in terms of the basis states, so that

$$|j\rangle = \sum_m C_{jm} |m\rangle_0 \ . \tag{9}$$

In order to calculate the intensity and polarization of the localized exciton photoluminescence we explore the following set of steady-state rate equations for the level populations f_j:

$$\left(\frac{\partial f_j}{\partial t}\right)_{rec} + \left(\frac{\partial f_j}{\partial t}\right)_{s.r.} + G_j = 0 \ , \tag{10}$$

$$\left(\frac{\partial f_j}{\partial t}\right)_{rec} = -\frac{1}{\tau_j} f_j \ , \ \frac{1}{\tau_j} = \frac{1}{\tau_r}\left(|C_{j,1}|^2 + |C_{j,-1}|^2\right) + \frac{1}{\tau_0} \ , \tag{11}$$

$$\left(\frac{\partial f_j}{\partial t}\right)_{s.r.} = -\sum_{j' \neq j}\left(\frac{f_j}{T_{j'j}} - \frac{f_{j'}}{T_{jj'}}\right) \ , \tag{12}$$

$$\frac{1}{T_{j'j}} = \frac{w_{j'j}}{\tau_s} \sum_{m'm} \eta_{m'm} |C_{jm} C_{j'm'}|^2 \ , \tag{13}$$

$$w_{j'j} = \begin{cases} 1 & \text{if } E_{j'} < E_j \ , \\ exp[-(E_{j'} - E_j)/k_B T] & \text{if } E_{j'} > E_j \end{cases} \ , \tag{14}$$

$$G_j = G_r \left|\sum_m C_{jm} M_m\right|^2 + G_0 \ , \ M_{\pm 1} = (e_x \pm i e_y) \ , \ M_{\pm 2} = 0 \ . \tag{15}$$

Here τ_r and τ_0 are the radiative and non-radiative lifetimes introduced in the previous section, $\eta_{mm'} = \delta_{|m-m'|,1}$ or $\delta_{|m-m'|,3}$ depending on whether the interlevel transitions are connected with spin-flips of an electron or a hole within the exciton. In our calculation we considered the latter possibility. The factor $w_{j'j}$ takes into account the difference in transfer rates for transitions from lower to higher levels and *vica versa*. For type II superlattices, the splittings $|E_{j'} - E_j|$ are small in comparison to the thermal energy $k_B T$ even for $T = 2$ K and one can put $w_{j'j} = 1$. For type I superlattices, the exchange interaction energy is comparable with the liquid helium temperature and the factors $w_{j'j}$, $w_{jj'}$ can noticeably differ from each other. The positive coefficients G_r and G_0 are proportional to the initial light intensity. They describe the generation rates (direct optical excitation or transitions from higher excitonic states) respectively polarization-dependent and -independent (e is the initial polarization unit vector). Under exactly resonant excitation $G_0 \ll G_r$, the opposite inequality takes place in the case of non-resonant photoexcitation of free carriers far into the band. For quasi-resonant (or close-to-edge) excitation, G_r and G_0 are expected to be of the same order of magnitude. The intensities of the photoluminescence circularly-polarized components are given by

$$I_{\pm} \propto \sum |C_{j,\pm 1}|^2 f_j \ . \tag{16}$$

Note that the above rate equations are valid provided the splittings $|E_{j'} - E_j|$ ($j \neq j'$) exceed the energy

uncertainty characterized by the parameter $\hbar(\tau_0^{-1} + \tau_r^{-1} + \tau_s^{-1})$. Otherwise one should apply the exciton spin-density-matrix formalism.

Fig.3 shows the total intensity, $I = I_+ + I_-$, and the degree of circular polarization, $P_c = (I_+ - I_-)/I$, of the photoluminescence as a function of the longitudinal magnetic field under unpolarized quasi-resonant optical excitation. The values of parameters used in the calculation are given in the figure caption. Due to the zero-field splitting δ_2 of the radiative doublet (see inset in Fig.3a) two level-anticrossing signals are clearly seen both in Fig.3a and Fig.3b. Physically, there are two independent reasons leading to the resonant behaviour of I and P_c: (1) the difference between the generation rates, $2(G_r + G_0)$ and $2G_0$, to the radiative ($m = \pm 1$) and non-radiative ($m \pm 2$) states, (2) the difference between the lifetimes, $\tau_0\tau_r/(\tau_0 + \tau_r)$ and τ_0, of these two pairs of states. If the reason 1 is dominant then the anticrossing is manifested by a resonant decrease in intensity and by an appearance of positive/negative nonthermal circular polarization respectively for the lower and higher radiative levels. On the contrary, if the reason 2 is more important which is the case for the parameters chosen in Fig.3 one should observe an increasing intensity and negative/positive P_c respectively for the lower- and higher-field anticrossings. This is in agreement with the experimental data presented in [11]. Under optical excitation with circularly polarized light, the anticrossing signal is superimposed on the smooth curve $P_c(B)$ arising due to optical orientation of exciton angular momenta (the inset in Fig.3b). Thus, the derived theory explains the observed[11] variation of P_c with magnetic field and predicts resonant changes in intensity by a few percent.

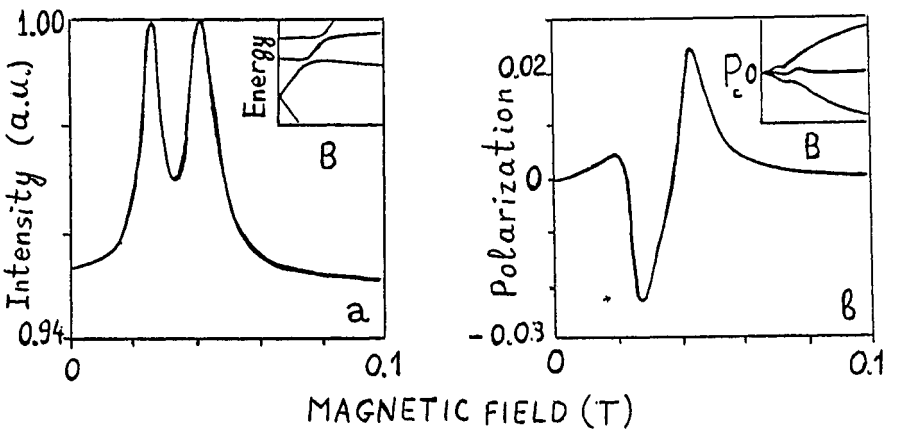

Fig. 3. The calculated magnetic-field dependences of photoluminescence intensity (a) and circular polarization (b) under quasi-resonant unpolarized optical excitation. The parameters used are: $g_e^{\parallel} = 2.08, 3g_h = 2.5, \delta_0 = 4.5\mu eV, \delta_2 = 2\mu eV, \delta_1 = 0$ (for the GaAs/AlAs superlattice 17.4 Å/26 Å [4]), $G_r = G_0, \tau_0/\tau_r = 4, \tau_s/\tau_0 \gg 1, |E_{j'} - E_j| \ll k_BT$ (type II superlattice, the unthermalized quartet). The insets show: (a) the energy-level diagram for the heavy-hole exciton and (b) the photoluminescence circular polarization for unpolarized, left (σ_-) and right (σ_+) circularly polarized excitation[9].

4. RESONANT RAMAN SCATTERING DUE TO ACCEPTOR-BOUND-HOLE SPIN-FLIPS

In this section we consider spin-polarized excitons acting as intermediate states in Raman scattering by spin flips of acceptor-bound holes observed in p-type GaAs/$Al_zGa_{1-z}As$ multiple quantum wells[12]. The experiment was performed in the backscattering Faraday configuration $z(\sigma_\eta, \sigma_\lambda)\bar{z}$, z being parallel to the heterostructure growth direction and $\eta = \pm$, $\lambda = \pm$ denoting the circular polarization of the exciting and scattered light respectively. The spin-flip Raman scattering (SFRS) under consideration is related to transitions within the magnetic-field-split ground state of the neutral acceptor and involves the angular-momentum flips $+3/2 \to -3/2$ or $-3/2 \to +3/2$ of a hole bound to an acceptor. The effect exhibits resonance behaviour and the scattering efficiency is significant only within a narrow frequency region between the low-energy edge of the photoluminescence spectrum and the fundamental-absorption edge of the type I heterostructure (Fig.4). The polarization of both the Stokes and anti-Stokes components was found to depend on the excitation energy, and at least two different mechanisms were identified to contribute to the bound-hole-related SFRS. As well as in the previous sections the following theoretical considerations are based on the selection rules for optical excitation (and emission) of $e1 - hh1$ excitons in the GaAs/AlGaAs quantum well: transition to the states $|-1/2, 3/2\rangle$ and $|1/2, -3/2\rangle$ are allowed respectively for σ_+ and σ_- polarizations and the states $|1/2, 3/2\rangle$ and $|-1/2, -3/2\rangle$ are inactive in the dipole approximation. Here in the notation $|s, m\rangle$ the first and second symbols indicate the projection of the electron and hole spin on the z axis.

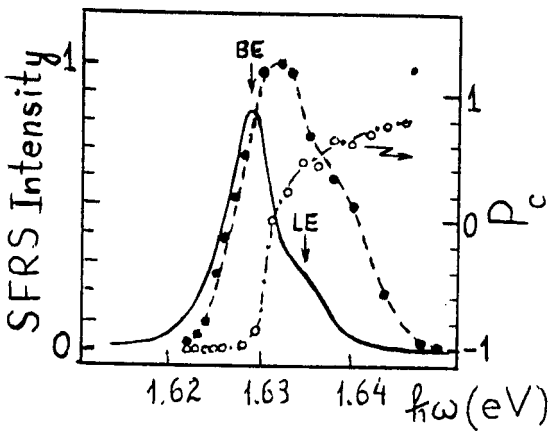

Fig. 4 Resonance profile of the SFRS efficiency for the $z(\sigma_-, \sigma_+ + \sigma_-)\bar{z}$ configuration in a magnetic field B = 10 T (dashed line, full dots). Photoluminescence spectrum of the multiple-quantum-wells 46/110 also for B = 10 T and excitation at $\hbar\omega = 1.7$ eV (solid line). The circles and dashed-dotted line show the dependence of the circular polarization, P_c, on the initial phonon energy under circularly-polarized excitation. (From [12])

Under excitation at the *high-energy edge*, both Stokes and anti-Stokes lines are observed in the parallel $z(\sigma_\eta, \sigma_\eta)\bar{z}$ configurations with their intensities being independent on the sign of η. The corresponding scattering process (process B in the notations of [12]) includes three stages: (B1) Absorption of a σ_η photon followed by formation of a three-particle complex consisting of a resonantly photoexcited spin-polarized exciton $|-\eta 1/2, \eta 3/2\rangle$ and an equilibrium hole bound to an acceptor neighboring the exciton localization area. (B2) As a result of the hole-hole "flip-stop" interaction

$$m, m_A \rightarrow m, -m_A$$

the acceptor-bound hole changes its sign from $m_A = \pm 3/2$ to $-m_A$ whereas the spin m of the hole in the exciton remains unchanged. (B3) Emission of a σ_η secondary photon by the localized exciton $|-\eta 1/2, \eta 3/2\rangle$.

The flip-stop interaction operator accounting for the process B can be written as

$$\mathcal{H}_{f-s} = \sigma_z^h(\Delta_+\sigma_+^A + \Delta_-\sigma_-^A), \tag{17}$$

where Δ_+ and Δ_- are complex-conjugate coefficients, $\sigma_\pm^A = \sigma_x^A \pm i\sigma_y^A$, σ_α^h and σ_β^A are the analogs of the Pauli matrices for a $\pm 3/2$ hole in the localized exciton (h) or at the acceptor (A). The operator (17) is similar to the contribution of $J'_{xz}S_{ix}S_{jz} + J'_{yz}S_{iy}S_{jz}$ to the spin-spin Hamiltonian of the magnetic ions that induces transitions with $\Delta m_i = \pm 1$, $\Delta m_j = 0$, where i and j are numbers of the ions and m_i, m_j are the eigenvalues of the spin operators S_{iz}, S_{jz}. In the axial approximation [13], $\Delta_\pm = f(\rho)\rho_\pm^3$, where $\rho_\pm = \rho_x \pm i\rho_y$ and (ρ_x, ρ_y) is the two-dimensional vector connecting the acceptor site with the center of localization of the exciton hole. The cubic dependence of $\Delta_\pm$ on $\rho_\pm$ can be understood taking into account that in the process B the acceptor-bound-hole changes the z component of its angular momentum by ± 3 and the photon angular-momentum projection holds unchanged.

At the *low-energy edge* of the SFRS resonance profile, Stokes and anti-Stokes lines are observed in the crossed $z(\sigma_\pm, \sigma_\mp)\bar{z}$ configurations respectively (process A in [12]). In the recent paper [14] it has been unambiguously shown that excitons bound to neutral acceptors (A^0X complexes) contribute to this scattering. The A^0X complexes act as resonant intermediate states and scattering occurs due to an additional acoustic-phonon-assisted spin flip of an electron in the exciton. Thus, the whole scattering process looks as follows. The σ_η circularly polarized light converts $-\eta 3/2$ neutral acceptors into $|A^0X, s\rangle$ complexes with the electron uncompensated spin $s = -\eta 1/2$ (stage A1). The generation rate is proportional to the equilibrium population, f_m, of the neutral acceptor state with the spin $m = -\eta 3/2$. The spin structure of the Kramers-conjugate states $|A^0X, s\rangle$ ($s = \pm 1/2$) is given by

$$|A^0X, s\rangle = |+\frac{3}{2}, -\frac{3}{2}; s\rangle + \frac{3}{4}\frac{\Delta_{hh}}{\Delta_C}|+\frac{1}{2}, -\frac{1}{2}; s\rangle - \frac{\sqrt{3}}{2}\frac{\Delta_{eh}}{\Delta_C}|3s, -s; -s\rangle\,. \tag{18}$$

Here we denote by $|m_1, m_2; s\rangle$ the state with hole angular momenta m_1, m_2 and electron spin s, Δ_{hh} and Δ_{eh} are the constants of hole-hole and electron-hole exchange interaction, Δ_C is the zero-magnetic-field splitting between the $\pm 3/2$ and $\pm 1/2$ neutral acceptor levels due to the quantum confinement effect. While deriving Eq.(18) it was assumed that the constants Δ_{hh} and Δ_{eh} are small as compared with the value of Δ_C. The next stage A2 is the spin-flip $|A^0X, s\rangle \rightarrow |A^0X, -s\rangle$ due to absorption or emission of an acoustic phonon. The most probable mechanism of the spin-lattice relaxation in A^0X complexes is determined by the admixture of the $|3s, -s; -s\rangle$ state in Eq.(18). At the final stage, A3, the A^0X complex annihilates with the emission of a $\sigma_{-\eta}$ photon and the remaining bound-hole finds itself in the inverted state $\eta 3/2$. It follows then that, for a positive hole g-factor and in a magnetic field directed along the z axis, the Stokes scattering occurs in the $z(\sigma_+, \sigma_-)\bar{z}$ configuration and the anti-Stokes line should be present only in the $z(\sigma_-, \sigma_+)\bar{z}$ spectrum, in agreement with the experiment.

Another important consequence is that, in contrast to the process B where the Raman shift is given by $\Delta E = 3g_A\mu_0 B_z$ (g_A is the acceptor-bound hole g-factor), the shift for the process A includes the Zeeman splitting of the

electron spin states in the A^0X complex: $\Delta E = (3g_A - g_e^{\parallel})\mu_0 B_z$. This has been verified in experiments[14] at a tilted magnetic field in which, in addition to the acoustic-phonon-assisted scattering, no-phonon SFRS becomes allowed since the electron in the A^0X complex can change its spin due to Zeeman interaction with the in-plane field component. The main result of measurements at tilted magnetic fields is the appearance of an additional Raman line under resonant excitation of A^0X complexes. Thus the Raman technique enables one to measure directly both the neutral-acceptor and electron g-factors as a function of the quantum well width. For the $GaAs/Al_{0.33}Ga_{0.67}As$ multiple-quantum-well structures with the layer thicknesses 46/110 Å, 72/110 Å and 102/110 Å the following values of the g-factors has been found[14]: $3g_A = 2.4$; 2.18; 2.09 and $g_e^{\parallel} = 0$; - 0.11; - 0.23 .

In addition to the strongest $\pm 3/2 \rightarrow \mp 3/2$ SFRS lines Sapega et al.[14] have observed two other lines. Their polarization properties and magnetic-field behavior indicate that they originate from the $+3/2 \rightarrow -1/2$ and $-3/2 \rightarrow 1/2$ interlevel transitions with the Raman shift

$$\Delta(\pm 3/2 \rightarrow \mp 1/2) = \Delta_C \mp g_A \mu_0 B\left(\frac{1}{2}\sqrt{\cos^2\phi + 4\sin^2\phi} + \frac{3}{2}\cos\phi\right),$$

where ϕ is the angle between $\mathbf{B}$ and z. The interlevel scattering can be described taking into account the hole-hole exchange interaction in the A^0X complex and an admixture of $\pm 1/2$ holes in the ground state presented by Eq.(18). For the above three samples the measured values of the 'crystal-field' splitting Δ_C are equal respectively to 7.3; 3.5 and 2 meV [14].

5. OPTICAL ORIENTATION OF HOT EXCITONS UNDER DOUBLE 2s-1s RESONANCE CONDITIONS

Optical orientation methods can be helpful to analyze mechanisms of doubly-resonant secondary emission of semiconductors. In optical spectroscopy the double resonance is defined as enhancement in the intensity of secondary emission under conditions where (i) the energies, $\hbar\omega$ and $\hbar\omega'$, of the incident and secondary photons coincide with those of two interband excitations (excitons) and (ii) the difference $\hbar(\omega - \omega')$ equals to the energy of one or few optical phonons. This effect which can be described in terms of both resonant Raman scattering and resonant photoluminescence has been observed in bulk materials (see [15] and references therein) as well as in quantum-well structures[16,17].

In [16,17] resonant states for incoming and outgoing channels were 1s-excitons attached to different size-quantized subbands or to different Landau levels. In [3] the double optical resonance has been observed on the states $e1-hh1(2s)$ and $e1-hh1(1s)$ belonging to the same excitonic series and related to the lowest electron and hole subbands. CdTe-based quantum well srtuctures were chosen for the observation of the 2s-1s resonance because of the following reasons: (1) In CdTe, the energy of a longitudinal optical (LO) phonon is relatively low: $\hbar\Omega_{LO} = 21$ meV , (2) In quantum wells $CdTe/Cd_{1-x}Mn_xTe$ (or $CdTe/Cd_{1-x}Mg_xTe$) the energy difference $\hbar\omega_{21}$ between the 2s and 1s exciton levels remarkably increases as a result of the quantum confinement effect and differs from $\hbar\Omega_{LO}$ just by a few meV. (3) In the magnetic field oriented along the growth axis, z, the 2s exciton level undergoes a strong diamagnetic blue shift and the condition $\omega_{21} = \Omega_{LO}$ is fulfilled in a moderate field $B < 10T$. The double 2s-1s resonance has been observed in backscattering Faraday geometry for circularly polarized analyzer and polarizer. In both photoluminescence (PL) and photoluminescence excitation (PLE) spectra the intensity of the sharp 1LO-replica has been found to increase rapidly with tuning to the double resonance conditions (Fig.5). An important fact is that a strong 1LO-line has been observed not only in parallel circular polarizations but also in the crossed $z(\sigma_+,\sigma_-)\bar{z}$ or $z(\sigma_-,\sigma_+)\bar{z}$ configuration.

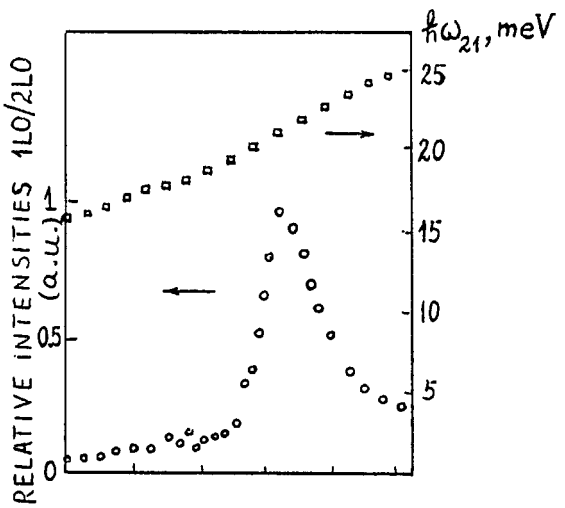

Fig. 5 The magnetic field dependence (circles) of the ratio between intensities of the 1LO- and 2LO- lines under double 2s-1s resonance observed in the $CdTe/Cd_{0.86}Mn_{0.14}Te$ 85 Å/95 Å multiple-quantum-well structure. Squares show the 2s-1s energy distance as a function of the magnetic field. (From [3])

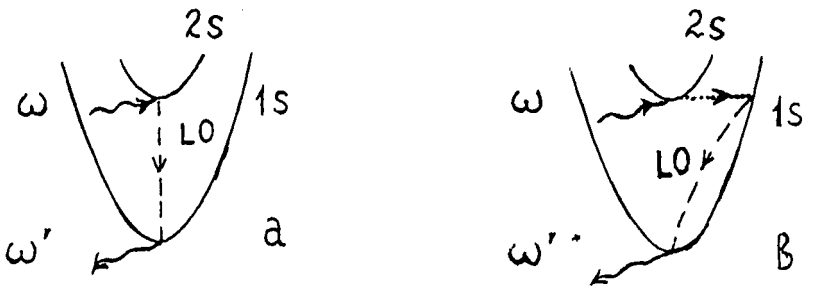

Fig. 6 Schematic representation of two possible mechanisms for doubly-resonant 2s-1s 1LO-assisted secondary emission.

Let us consider two possible mechanisms of the doubly-resonant 2s-1s secondary emission. The both are illustrated in Fig.6. For the direct doubly-resonant one-phonon Raman scattering (see the two-step process of Fig.6a), optical excitation of the 2s exciton is followed by the LO-phonon-assisted transition to the bottom of the 1s-exciton subband and then by emission of a photon from the 1s state. However the analysis shows that the vertical transition $2s \rightarrow 1s + LO$ is ineffective. Really, in a bulk semiconductor, such a transition is forbidden in the dipole approximation, i.e. the corresponding matrix element $V^{LO}_{1s,2s} \propto q_z$, where q_z is the scattered wave vector (the difference between wave vectors of the incident and secondary photons). Remind that by similar reason in resonant spectra of secondary emission of perfect crystals the 1LO-line is much weaker than the 2LO line. On the other hand, in the two-dimentional approximation the exciton envelope function is factorized so that

$$\Psi_{n,s} = f_{n,s}(\rho)\varphi_{e1}(z_e)\varphi_{h1}(z_h) \tag{19}$$

with the same single electron and hole envelopes $\varphi_{e1}, \varphi_{h1}$ for 1s and 2s states. Here $f_{n,s}(\rho)$ is the envelope function describing the relative electron-hole motion in the (x,y) plane and $\rho = [(x_e - x_h)^2 + (y_e - y_h)^2]^{1/2}$. The condition of orthogonality between $f_{1s}(\rho)$ and $f_{2s}(\rho)$ immediately makes zero the matrix element $V^{LO}_{1s,2s}$ since for backscattering of normally-incident light the exciton-phonon interaction operator is ρ-independent. Thus, the value of $V^{LO}_{1s,2s}$ can be nonvanishing only due to the Coulomb-potential effect upon the electron or hole confinement along the z direction. Furthermore, for the direct process of Fig.6a the exciton polarization cannot undergo a remarkable change which contradicts to the presence of the strong 1LO-line in the spectra observed in the crossed circular polarizations.

The more realistic mechanism is illustrated in Fig.6b: the 2s-exciton is first scattered from the bottom of the 2s branch to the "hot" 1s states characterized by large in-plane center-of-mass wave vectors, $\mathbf{K}$, then it is multi-scattered by static random potential of the heterostructure and only afterwards emits a LO-phonon. Obviously the second mechanism has more grounds to be interpreted as a luminescence rather than Raman scattering. It should be mentioned that similar static scattering processes with a large momentum transfer were suggested by Kleinman et al.[16] and Gubarev et al.[15] in order to interpret their results on doubly resonant LO-phonon-assisted secondary emission respectively in GaAs/Al_xGa_{1-x}As quantum wells and bulk semimagnetic semiconductor $Cd_{0.95}Mn_{0.05}Te$.

According to the theory of resonant secondary emission in semiconductors (see [1]), for the process shown in Fig.6b the spectral intensity, $I(\omega', \omega)$, of the 1LO-phonon replica can be presented in the form

$$I(\omega', \omega) \propto \delta(\omega' - \omega + \Omega_{LO}) \sum_{\mathbf{K}ff'} S_{ff'}(\mathbf{K}, \omega') F_{ff'}(\mathbf{K}), \tag{20}$$

where

$$S_{ff'}(\mathbf{K}) \propto g_{1lm'}(\omega') \sum_{\mathbf{q}} (|M_{1lm'}(\mathbf{e}')|^2 \tau_{1lm'} V^{LO,\mathbf{q}}_{1lm',\mathbf{K}f} V^{LO,\mathbf{q}*}_{1lm',\mathbf{K}f'}) \tag{21}$$

and $F_{ff'}(\mathbf{K})$ is the hot 1s-exciton spin-density matrix which obeys the kinetic equation

$$\left[\frac{1}{\tau_s} + i(\omega_{\mathbf{K}f} - \omega_{\mathbf{K}f'})\right] F_{ff'}(\mathbf{K}) + \sum_{\mathbf{K}'} w_{\mathbf{K}'\mathbf{K}} [F_{ff'}(\mathbf{K}) - F_{ff'}(\mathbf{K}')] = G_{ff'}(\mathbf{K}) \tag{22}$$

with the generation matrix given by

$$G_{ff'}(\mathbf{K}) = C J_0 |M_{2s,m}(\mathbf{e})|^2 \Delta(\omega_{2s,m} - \omega, \Gamma_2) \tau_2 \frac{2\pi}{\hbar^2} D^{1s,2s}_{\mathbf{K}f,0m} D^{1s,2s*}_{\mathbf{K}f',0m} \delta(\omega_{1\mathbf{K}} - \omega). \tag{23}$$

The notations used are as follows: ω, J_0 and $\mathbf{e}$ are the incident light frequency, intensity and polarization unit

vector, ω' and $\mathbf{e}'$ refer to the secondary radiation,

$$\Delta(\omega_{2s,m}-\omega,\Gamma_2)=\frac{1}{\pi}\frac{\Gamma_2}{(\omega_{2s,m}-\omega)^2+\Gamma_2^2}, \tag{24}$$

$\omega_{2s,m}$ and Γ_2 are the resonance frequency and homogeneous broadening of the 2s-exciton , m is the exciton spin index. $D^{1s,2s}_{\mathbf{K}f,0m}$ is the matrix element of elastic scattering from the state $2s, K=0$ to the hot state $1s,\mathbf{K}f$ with the energy $\hbar\omega_{1\mathbf{K}f}$ and two-dimensional wave vector $\mathbf{K}$, the index f enumerates the hot-exciton sublevels. The 2s-exciton lifetime τ_2 is connected with Γ_2 and $D^{1s,2s}$ by the relations

$$\frac{1}{\tau_2}=2\Gamma_2=\frac{2\pi}{\hbar^2}\sum_{\mathbf{K}f}|D^{1s,2s}_{\mathbf{K}f,0m}|^2\delta(\omega_{1\mathbf{K}f}-\omega_{2s,m}). \tag{25}$$

$w_{\mathbf{K}',\mathbf{K}}$ is the probability rate for the elastic scattering $\mathbf{K}\to\mathbf{K}'$, τ_ε is the hot exciton lifetime with respect to inelastic processes, and $V^{LO,\mathbf{q}}_{1lm',\mathbf{K}f}$ is the matrix element for the transition $1s,\mathbf{K}f\to 1lm'$ accompanied by the emission of the LO-phonon with the wave vector $\mathbf{q}$. For simplicity we neglect the LO-phonon bulk dispersion and confinement energy and consider the phonon frequency Ω_{LO} as a constant. The index l enumerates the emitting weakly-localized and extended 1s-exciton states with the spin $m'=\pm1$ and lifetime $\tau_{1lm'}$, $g_{1lm'}(\omega')$ is the density of such states, the angle brackets in Eq.(21) indicate averaging over different states with the same excitation energy $\hbar\omega'$. $M_{2s,m}(\mathbf{e})$ and $M_{1lm'}(\mathbf{e}')$ are the matrix elements of the exciton-photon interaction. Since here we consider backscattering of normally-incident polarized light in the parallel or crossed circular configurations $M_{2s,m}(\mathbf{e})$ is non-zero for $m=\pm1$ respectively under σ_+ or σ_- excitation and similarly $M_{2s,m'}(\mathbf{e})$ is non-zero for m' corresponding to the detection polarization $\sigma_\pm$.

If the exciton energy $\hbar\omega_{1\mathbf{K}f}$ is spin-independent and spin-flip processes are neglected, then the polarization of the 1LO-line coincides with the initial light circular polarization. However, due to the long-range electron-hole exchange interaction, the exciton states $1\mathbf{K}f$ longitudinal and transverse with respect to the wave vector $\mathbf{K}$ are split with the splitting $\hbar\tilde{\Omega}(K)$ vanishing linearly with K as $K\to 0$ [18]. This results in the effective exciton spin relaxation described by the inverse spin-relaxation time [19]

$$\frac{1}{T_s}=\tilde{\Omega}^2(K)\frac{\tau^*}{1+(\Omega_0\tau^*)^2}, \tag{26}$$

where $\hbar\Omega_0$ is the magnetic-field-induced splitting between the exciton states with $m=1$ and $m=-1$ and τ^* is the momentum scattering time. Note that the bulk-exciton spin-relaxation due to the longitudinal-transverse splitting was considered by Pikus and Ivchenko[1] .

If the spin-relaxation time T_s is much smaller than the hot-exciton inelastic scattering time τ_ε the 1LO-line polarization is insensitive to the initial polarization while its intensity can depend on $\mathbf{e}$ via the factor $|M_{2s,m}(\mathbf{e})|^2$ in Eq.(23). Thus the observation of a remarkable 1LO-replica in the crossed (σ_+,σ_-) or (σ_-,σ_+) configuration is readily understood provided $T_s\le\tau_\varepsilon$.

The integral intensity $J(\omega)=\int d\omega' I(\omega',\omega)$ and integral photoexcitation intensity $J_{PE}(\omega')=\int d\omega I(\omega',\omega)$ are given by Eq.(20) where the δ-function is removed, ω and ω' satisfy the relation $\omega'=\omega-\Omega_{LO}$ and either ω or ω' is considered as a varying parameter. The frequency dependences $J(\omega')$, $J_{PE}(\omega)$ are determined by the function $S_{ff'}(\mathbf{K},\omega-\Omega_{LO})$ in Eq.(20), by the smeared δ-function in Eq.(23) and by inhomogeneous broadening. Qualitative analysis of the behaviour of $g_{1lm'}(\omega')$, $\tau_{1lm'}$ and $|M_{1lm'}(\mathbf{e}')|^2$ near the exciton band bottom $\omega_{1s,m'}$ shows that $S_{ff'}(\mathbf{K},\omega')$ should exhibit a sharp peak red-shifted from $\omega_{1s,m'}$ by $\delta\omega\approx\Delta(PL-PLE)$ and characterized by the width $2\gamma\le\Delta(PL-PLE)$. Here $\Delta(PL-PLE)$ is the Stokes shift between the PL peak excited in off-resonant conditions and the peak in the PLE spectrum taken at some frequency below the 1s free-exciton resonance (for the studied samples $\Delta(PL-PLE)\approx 0.9$ meV). Furthermore, let $P(\omega_{1s,m}-\bar{\omega}_{1s,m})$ be the statistical distribution of the frequency $\bar{\omega}_{1s,m}$ with maximum at the point $\bar{\omega}_{1s,m}$ and with the characteristic width $2\bar{\Gamma}$. If $\gamma\ll\Gamma_2,\bar{\Gamma}$ and fluctuations of the energy distance between the exciton levels 2s and 1s are negligible as compared with Γ_2 and $\bar{\Gamma}$ then the dependences of $J_{PE}(\omega')$ for the 1LO-phonon replica upon the frequency ω' and 2s-1s spacing, ω_{21}, are governed respectively by the parameters $\bar{\Gamma}$ and Γ_2 through the factors $P(\omega'-\bar{\omega}_{1s,m'})$ and $\Delta(\omega_{21}+\delta\omega-\Omega_{LO},\Gamma_2)$. Thus, from the resonance profile of Fig.5 one can find $2\hbar\Gamma_2=2.6$ meV or $\hbar\Gamma_2=1.3$ meV for homogeneous broadening of the 2s-exciton resonance. The inhomogeneous broadening found from the width of the $e1-hh1(1s)$ peak in the PLE spectrum equals to $2\hbar\bar{\Gamma}=2.1$ meV and is comparable with $2\hbar\Gamma_2$.

6. CONCLUSION

Thus, the optical spectroscopy of spin-polarized excitons is an effective tool to propose and investigate microscopic mechanisms of the observed optical processes and to measure the exciton fine-structure parameters and damping rate as well as electron and hole g-factors.

The author is grateful to P.Lavallard, A.Yu.Kaminskii, D.N.Mirlin and D.R.Yakovlev for useful discussions.

7. REFERENCES

1. G.E.Pikus, E.L.Ivchenko, "Optical orientation and polarized luminescence of excitons in semiconductors", In: *Excitons*, ed. by E.I.Rashba and M.D.Sturge, North-Holland, 1982, pp.205–266.

2. W.M.Chen, M.Godlewski, B.Monemar, J.P.Bergman, "Steady-state level-anticrossing for bound-exciton triplets associated with complex defects in semiconductors", *Phys. Rev. B*, vol. 41, pp. 5746–5755, 1990.

3. D.R.Yakovlev, W.Ossau, A.Waag, G.Landwehr. "Double 2s-1s optical resonance in quantum-well structures", To be published.

4. C.Gourdon, P.Lavallard, "Fine structure of heavy excitons in GaAs/AlAs superlattices", *Phys. Rev. B*, vol. 46, pp. 4644–4650, 1992.

5. E.L.Ivchenko, V.P.Kochereshko, A.Yu.Naumov, I.N.Uraltsev, P.Lavallard, "Magnetic-field-effects on photoluminescence polarization in type II GaAs/AlAs superlattices", *Superlatt. Microstruct.*, vol. 10, pp. 497–501, 1991.

6. H.W. van Kesteren, E.C.Cosman, W.A.J.A. van der Poel, C.T.Foxon, "Fine structure of excitons in type-II GaAs/AlAs quantum wells", *Phys. Rev. B*, vol. 41, pp. 5283–5292, 1990.

7. E.L.Ivchenko, A.Yu.Kaminskii, I.L.Aleiner, "Exchange spliting of excitonic levels in type I and II superlattices", *JETP*, vol. 77, pp. 609–616, 1993.

8. G.Edwards, J.C.Inkson, "Hole states in GaAs/AlAs heterostructures and the limitations of the Luttinger model", *Solid State Commun.*, vol. 89, pp. 595–599, 1994.

9. E.L.Ivchenko, A.Yu.Kaminskii, "Optically detected anticrossing of excitonic levels in superlattices in a magnetic field" , In: Nanostructures: Physics and Technology, *Proc. Int. Symposium*, St.Petersburg, Russia, 1994, pp. 58–61.

10. C.Gourdon, D.Yu.Rodichev, P.Lavallard, G.Bacquet, R.Planel, "Anisotropic exciton states in GaAs/AlAs superlattices in zero and non-zero magnetic field", *J. de Physique IY*, vol. 3, Suppl. JPII, C5, pp. 183–186, 1993.

11. P.G.Baranov, I.V.Mashkov, N.G.Romanov, P.Lavallard, R.Planel, "Optically detected magnetic resonance of excitons and carriers in pseudodirect GaAs/AlAs superlattices", *Solid State Commun.*, vol. 87, pp. 649–654, 1993.

12. V.F.Sapega, M.Cardona, K.Ploog, E.L.Ivchenko, D.N.Mirlin, "Spin-flip Raman scattering in $GaAs/Al_zGa_{1-z}As$ multiple quantum wells", *Phys. Rev. B*, vol. 45, pp. 4320–4326, 1992.

13. E.L.Ivchenko, "Exchange interaction and scattering of light with reversal of the hole angular momentum at an acceptor in quantum-well structures", *Sov. Phys. Solid State*, vol. 34, pp. 254–260, 1992.

14. V.F.Sapega, T.Ruf, M.Cardona, K.Ploog, E.L.Ivchenko, D.N.Mirlin, "Resonant Raman scattering due to bound-carrier spin flip in $GaAs/Al_zGa_{1-z}As$ quantum wells", *Phys. Rev. B*, vol. 50, 15 July, 1994.

15. S.I.Gubarev, T.Ruf, M.Cardona, "Doubly resonant Raman scattering in the semimagnetic semiconductor $Cd_{0.95}Mn_{0.05}Te$", *Phys. Rev. B*, vol. 43, pp. 1551–1554, 1991.

16. D.A.Kleinman, R.C.Miller, A.C.Gossard, "Doubly resonant LO-phonon Raman scattering observed with $GaAs$-$Al_zGa_{1-z}As$ quantum wells", *Phys. Rev. B*, vol. 35, pp. 664–674, 1987.

17. F. Calle, J.M. Calleja, F. Meseguer, C. Tejedor, L. Vina, C. Lopez, C. Ploog, "Double Raman resonances induced by a magnetic field in GaAs-AlAs multiple quantum wells", *Phys. Rev. B*, vol. 44, pp. 1113–1117, 1991.

18. L.C.Andreani, F.Bassani, "Exchange interaction and polariton effects in quantum-well excitons", *Phys. Rev. B*, vol. 41, pp. 7536–7544, 1990.

19. M.Z.Maialle, E.A. de Andrada e Silva, L.J.Sham, "Exciton spin dinamics in quantum wells", *Phys. Rev. B*, vol. 47, pp. 15776–15788, 1993.